Molecular Therapy
Methods & Clinical Development
Original Article

Systemic delivery of AAV5, AAV8, and AAV9 packaging a C5-12-microdystrophin-FLAG expression cassette in non-human primates

Mengping Liu,[1] Erica Cook,[1] Yanshan Dai,[1] Erich Ehlert,[2] Francois du Plessis,[2] Jacek Lubelski,[2] Bogdan G. Sleczka,[1] Petia Shipkova,[1] Zhuyin Li,[1] Joshua Gamse,[1] David Gordon,[1] Leonard P. Adam,[1] Paul C. Levesque,[1] and Glen B. Banks[1]

[1]Bristol Myers Squibb, 3551 Lawrenceville Road, Princeton, NJ 08540, USA; [2]uniQure, Paasheuvelweg 25a, 1105 BP Amsterdam, the Netherlands

Safely achieving therapeutic expression levels with adeno-associated virus (AAV) gene therapy is a significant challenge for treating the large muscle mass in humans. Non-human primates (NHPs) provide a more accurate assessment of the feasibility of achieving an effective and safe dose than rodents. Here, we compared a single systemic administration of AAV5, AAV8, or AAV9 in NHPs, each packaging the C5-12-microdystrophin-FLAG expression cassette. At 1 month post-dose, we compared tissue vector genomes, mRNA, and microdystrophin-FLAG protein levels by meso-scale discovery-enzyme-linked immunosorbent assay, liquid chromatography-mass spectrometry, and immunofluorescence. The C5-12 promoter was highly selective for heart and skeletal muscles, when compared to off-target tissues such as peripheral blood mononuclear cells, lung, liver, and kidney. AAV8 led to higher levels of microdystrophin-FLAG mRNA and protein in the cardiac ventricles and skeletal muscles when compared to AAV5 or AAV9. The AAV8-microdystrophin-FLAG led to ∼20% of wild-type NHP dystrophin protein expression levels and was located on the sarcolemma of ∼40% of skeletal muscles fibers and ∼15% of left ventricular cardiomyocytes. Hematology, serum chemistry, and pathology were unremarkable. Thus, a systemic dose of ∼1.18×10^{14} vector genomes/kg AAV8 is predicted to be safe and efficacious for treating Duchenne muscular dystrophy (DMD) but has significant room for improvement.

INTRODUCTION

Gene therapies are diverse modalities that use genes to treat, prevent, or cure a disease.[1] Adeno-associated virus (AAV) can deliver a rationally designed therapeutic DNA expression cassette that can form stable episomes in muscle nuclei for years, with the potential to provide a one-shot long-term treatment of serious unmet diseases.[2] AAV gene therapy is a promising approach for treatment of striated muscle disorders, including various muscular dystrophies, cardiomyopathies, and heart failure.[3–7] However, safely achieving sufficient therapeutic expression levels is a significant challenge for the treatment of the large muscle mass in humans.[8]

Non-human primates (NHPs) are particularly important for translating pre-clinical proof-of-concept studies.[9,10] NHPs are generally utilized to assess dose projection, target engagement, pharmacokinetics, pharmacodynamics, and various toxicology parameters before human safety trials.[9] Specifically, for AAV gene therapies, NHPs provide a translatable model to define the suitability of systemic delivery of the gene therapy to achieve an effective dose, defined by the relationship between AAV vector genomes (VG), mRNA, protein levels, and biodistribution (proportion of target cells expressing the therapeutic) that are required for therapeutic benefit in a preclinical model. Together, these studies provide a more accurate assessment of the feasibility for achieving an effective and safe dose to treat the target disease in humans.

AAV serotypes bind different cell surface receptors that define their relative tropism for certain tissues and can also impact the successful delivery of the DNA to the nucleus once inside the cell.[11–15] The tropism of AAV8 and AAV9 for striated muscle makes them the capsids of choice in clinical trials and approved therapeutics.[5,7,16–18] AAV5 is ancestrally distinct from other capsids, and its tropism for striated muscle in large animals is less clear.[19] AAV5 is an attractive serotype to study given its proven safety in humans[20] and the potential to treat more patients due to lower global seroprevalence of neutralizing antibodies (nAbs).[21]

The therapeutic expression cassette is also critical for safely achieving sufficient levels of expression to treat disease. Various muscle-specific promoters have been generated to achieve cardiac-selective expression, skeletal muscle-selective expression, or striated muscle-selective expression.[22–28] The C5-12 promoter is potentially one of the most active in striated muscle,[22] but less is known about its selectivity in NHPs.

Received 9 August 2024; accepted 14 January 2025;
https://doi.org/10.1016/j.omtm.2025.101411.

Correspondence: Glen B. Banks, Bristol Myers Squibb, 3551 Lawrenceville Road, Princeton, NJ 08540, USA.
E-mail: gbanks@solidbio.com

Table 1. Percent luciferase expression relative to nAb negative control

nAb test, timing	AAV5 (1.18×10^{14} VG/kg)			AAV8 (1.18×10^{14} VG/kg)		AAV9 (1.18×10^{14} VG/kg)			AAV9 (2×10^{14} VG/kg)	
Group ID	1101	1102	1103	2101	2102	3101	3102	3103	4101	4102
AAV5										
Pre-treat	51	87	81	51	59	106	156	94	78	60
Day 15	1[a]	1[a]	2[a]	91	101	87	94	93	107	95
Day 29	1[a]	1[a]	0[a]	93	121	118	116	117	89	62
AAV8										
Pre-treat	87	34[a]	101	102	131	82	88	114	111	116
Day 15	110	139	88	0[a]	4[a]	111	81	121	102	85
Day 29	74	148	99	2[a]	6[a]	107	106	91	94	76
AAV9										
Pre-treat	86	2[a]	18[a]	86	37	59	93	100	69	65
Day 15	114	84	111	85	18[a]	0[a]	1[a]	6[a]	1[a]	1[a]
Day 29	113	94	97	82	44[a]	1[a]	2[a]	2[a]	0[a]	1[a]

nAbs in the serum lead to low percentages of luciferase expression.
[a]nAb in the serum lead to low percentages of liciferase expression.

Duchenne muscular dystrophy (DMD) is a severe skeletal muscle wasting disease, with dilated cardiomyopathy caused by mutations in dystrophin.[29] Dystrophin replacement gene therapies require rationally designed miniaturized dystrophins to accommodate the limited packaging capacity of AAV.[3,30] Here, we utilized an epitope-tagged microdystrophin transgene that has previously been shown to be safe in NHPs when delivered intramuscularly or by local vascular administration at high doses.[31]

In this study, we had two primary goals. First, we assessed the tropism of AAV5, AAV8, and AAV9 in in the cynomolgus monkey (*Macaca fascicularis*), when the AAV was manufactured utilizing the baculovirus expression vector system (BEVS).[32,33] Second, we examined the tissue selectivity and activity of the striated muscle C5-12 promoter in NHPs, where the striated muscles resemble the fiber types found in humans.[34] Here, we found that each serotype effectively transduced striated muscle, and the C5-12 promoter was highly selective for both cardiac and skeletal muscles in NHPs.

RESULTS

This was a single-dose exploratory intravenous study in NHPs (study DN20027) with a 4-week post-dose termination. We compared BEVS-derived AAV5, AAV8, and AAV9, each packaging the same expression cassette at a dose of 1.18×10^{14} VG/kg AAV5 ($n = 3$), 1.18×10^{14} VG/kg AAV8 ($n = 2$), and 1.18×10^{14} VG/kg AAV9 ($n = 3$) or 2×10^{14} VG/kg AAV9 ($n = 2$). The expression cassette contains a synthetic striated muscle-specific C5-12 promoter, a human microdystrophin containing the actin-binding domain, hinge 1, spectrin-like repeats 1–3, hinge 2, spectrin-like repeat 24, hinge 4, and the cysteine-rich region originally designed by the Chamberlain laboratory.[30,35] and adapted to generate ELEVIDYS by Sarepta Therapeutics.[17,26] The miniaturized dystrophin was conjugated to a C-terminal FLAG tag that was well tolerated in NHPs after limb infusion.[31] The expression cassette has a synthetic poly(A), but no 5′ UTR or 3′ UTR and is ∼4.4 kb, including inverted terminal repeats (ITRs).

Selecting NHPs with low levels of nAbs

Pre-treatment serum samples from 15 NHPs were screened by a cell-based nAb assay and an enzyme-linked immunosorbent assay (ELISA)-based total antibody assay (Tables 1 and S1). The cutoff for the nAb assay was luciferase activity that was inhibited by less than 50% of negative controls (10% fetal bovine serum; asterisk in Table 1). The positive controls were <50% in all 3 AAV serotype nAb assays. Five animals were excluded based on high levels of pre-treatment antibodies and therefore had no group assigned to them (Table S1). This resulted in 10 NHPs available for the study. Of these, 8 NHPs were identified to have low nAbs for all three tested AAV serotypes (Table 1). The remaining 2 NHPs (group IDs 1102 and 1103) had low total antibodies (tAbs) and nAbs for AAV5 but were neutralized by AAV8 and/or AAV9 and were therefore chosen to be in the AAV5 treatment cohort (Table S1).

Post-treatment serum samples from days 15 and 29 were analyzed in the cell-based nAb assay to determine the level of nAbs against AAV5, AAV8, and AAV9 serotypes. The post-treatment nAbs were specific to the administered serotype with no cross-reactivity, with only one exception being treatment group ID 2102, which was administered AAV8 but developed nAbs to AAV8 and AAV9. Interestingly, the AAV5 samples that were neutralized by AAV8 and/or AAV9 in pre-treatment (group IDs 1102 and 1103) were no longer neutralized by AAV8 or AAV9 post-treatment.

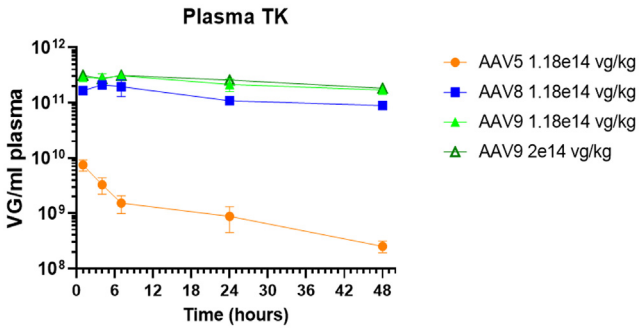

Figure 1. Plasma toxicokinetics (TK)

The mean ± SD of C5-12-microdystrophin-FLAG VG/1 mL of plasma extracted 1, 3, 6, 24, and 48 h post-dose. Note that the AAV5 VG was cleared faster than either AAV8 or AAV9.

Plasma toxicokinetics

To estimate the clearance of each AAV-C5-12-microdystrophin-FLAG, plasma concentrations of the AAV VG were measured up to 48 h after treatment (Figure 1). AAV5 was mostly cleared from the blood within ∼24 h, while AAV8 and AAV9 remained for a period longer than 48 h (Figure 1).[36]

Biodistribution and expression in the heart

We next measured the biodistribution and microdystrophin-FLAG expression in the heart. The highest VG levels were in the atria, but this translated to minimal levels of mRNA and no microdystrophin-FLAG protein in the left atria and low levels in the right atria (Figure 2). In other regions of the heart, a narrow range of $\sim 1 \times 10^5$ to 4×10^5 VG/μg genomic DNA (gDNA) led to a similarly narrow range between $\sim 1 \times 10^5$ and 6×10^5 mRNA copies/μg total RNA (Figure 2A). The mRNA translated to low levels of protein with no clear difference in translation between the tested serotypes (Figure 2B). However, AAV5 and AAV8 led to the highest expression in the left and right ventricles when compared to AAV9 at the same dose of 1.18×10^{14} VG/kg (Figures 2C and S1). Each AAV serotype had the highest expression in the ventricles, septum, and apex when compared to the atria (Figure 1C).

Biodistribution and expression in the skeletal muscles

The expression profile was different in skeletal muscles when compared to the heart. A narrow range between 1 and 2×10^5 VG/μg gDNA led to ∼10-fold higher levels of mRNA/μg total RNA in skeletal muscles when compared to the heart (Figures 3A and S2; unfortunately, we did not measure the AAV9-treated diaphragm samples). mRNA levels below $\sim 1 \times 10^6$ mRNA/μg total RNA led to low levels of microdystrophin-FLAG protein similar to that of the heart (Figure 3B). However, levels above $\sim 1 \times 10^6$ mRNA/μg total RNA led to 3- to 4-fold higher levels of microdystrophin-FLAG protein (Figure 3B). One of the NHPs treated with AAV8 (group ID 2102) had the highest levels of protein in the diaphragm, quadriceps, gastrocnemius, forearm, and tongue, but not mandible or esophagus (Figure 3C). Interestingly, this NHP also developed cross-reactive levels of nAbs to AAV9 (Table 1).

We also examined microdystrophin-FLAG protein expression by liquid chromatography-mass spectrometry (LC-MS) to measure the proportion of the endogenous full-length dystrophin levels. We compared the highest dose of AAV9 (2×10^{14} VG/kg) to AAV8 at 1.18×10^{14} VG/kg (Figure 3D). The results are consistent with AAV8 leading to more protein expression than AAV9, and these levels are approximately 20% of wild-type dystrophin levels with a dose of 1.18×10^{14} VG/kg AAV8 (Figure 3D).

Proportion of striated muscles expressing microdystrophin-FLAG

The proportions of cardiomyocytes and skeletal muscle fibers expressing microdystrophin-FLAG were examined by confocal microscopy with an automated algorithm to define a positive cell. Both α2-laminin and endogenous dystrophin immunofluorescence were used to mark the positive muscle membranes (Figure S3). Consistent with both the meso-scale discovery (MSD)-ELISA and LC-MS data, the AAV8 (1.18e14 VG/kg) led to the broadest expression of microdystrophin-FLAG when compared to the higher dose (2e14 VG/kg) of AAV9 (Figure 4).

Off-target tissues

As anticipated, the highest levels of VG were found in the liver (Figure 5A). The VG liver, lung, and peripheral blood mononuclear cells led to background levels of microdystrophin-FLAG protein (∼1,096 a.u.; Figures 5B and 5C). Only the kidney for AAV5 and AAV9 treatment and liver for AAV9 treatment had microdystrophin-FLAG protein levels marginally above baseline (Figure 5), showing the excellent selectivity of the C5-12 promoter for striated muscles.

DISCUSSION

Safely achieving therapeutic expression levels with AAV gene therapy is a significant challenge for treating the large muscle mass in humans.[8] NHPs provide a more accurate assessment of the feasibility of achieving an effective and safe dose to treat the target disease in humans.[9,10] Here, we found that AAV5, AAV8, and AAV9 generated using BEVS were each able to deliver the microdystrophin-FLAG therapeutic expression cassette to striated muscles and that the C5-12 promoter was highly selective for striated muscles.

The biodistribution and expression in NHPs differs substantially from those in rodents. For instance, AAV8 and AAV9 lead to higher expression in the heart compared to the skeletal muscles in rodents, with diaphragm being the lowest.[15,26] The opposite result was achieved in NHPs, where the highest expression is in skeletal muscles when compared to the heart, and the biodistribution and expression in the diaphragm were similar to those of the limb muscles. The better tropism in rodent hearts may be driven by species differences in AAV receptor sequences and/or by the higher heart rates (∼550 bpm) when compared to NHPs (60 bpm). Furthermore, AAV5 has poor tropism for striated muscles in rodents but was comparable to

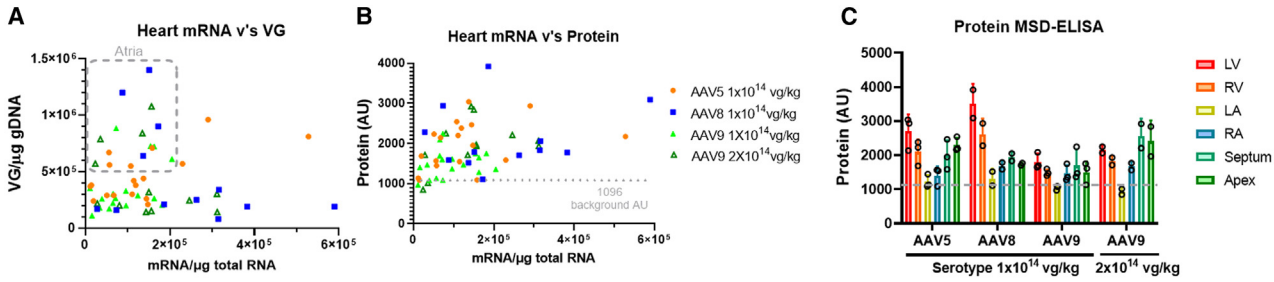

Figure 2. Expression and biodistribution in the heart after systemic delivery of AAV-C5-12-micordystrophin-FLAG

(A) The relationship of VG/µg gDNA versus mRNA/µg total RNA for each sample. Dashed box shows the atria samples with high VG levels but low mRNA levels. (B) The relationship of MSD-ELISA-quantified microdystrophin-FLAG protein levels versus mRNA/µg total RNA for each sample. The dashed line shows the average background arbitrary units from the MSD-ELISA. (C) The mean ± SD MSD-ELISA protein levels from each region of the heart, including LV (left ventricle), RV (right ventricle), LA (left atria), RA (right atria), septum, and apex.

AAV8 in NHP hearts.[11,37] The differences between rodents and NHPs underscore the importance of evaluating biodistribution and expression in large animals to extrapolate dose projections more accurately for humans.

Overall, systemic delivery of AAV8 led to better biodistribution and protein expression in striated muscles of NHPs when compared to AAV5 and AAV9. The VG in the tissues were similar between serotypes, and this may have resulted from the short timeline of this study (∼1 month) as it may require longer time periods to clear VG that did not effectively form stable concatemers in the nucleus. Comparisons of VG, mRNA, and protein levels clearly reveal that VG delivered by AAV8 led to more effective transcription of microdystrophin-FLAG mRNA, and this greater level of mRNA led to more muscle cells expressing more microdystrophin-FLAG protein. AAV8 is also superior to AAV9 in neonatal dog hearts.[16] The biology behind this is unclear. Perhaps one explanation is that AAV8 protects the VG from TLR9-mediated immune responses[12] better than either AAV5 or AAV9, but this would need to be tested.

The rational design of miniaturized muscle-specific promoters is important to accommodate the limited available DNA size that can package into AAV and to optimize expression in striated muscles to achieve efficacious doses of protein.[22–27] The miniaturization of creatine kinase promoters has been incorporated into rationally designed therapeutic expression cassettes to treat DMD.[23,38,39] Careful analyses of CK7 and MHCK7 revealed preferential expression in fast fiber types.[23] Most mouse skeletal muscles are fast 2b fiber types that are not found in humans.[34] We tested the C5-12 striated muscle-specific promoter because it has no fiber type preference.[22,28,40] Here, the C5-12 promoter led to highly selective striated muscle-specific expression in NHPs, with the only exception being low levels (just above background) in the kidney. While the biology behind the better translation of low levels of VG in skeletal muscles versus cardiac muscles is unclear, it is possible that the C5-12 promoter is more active in skeletal muscles than the heart or reflects the skeletal muscle syncytium.[41] Similarly, that the high level of VG in atria did not lead to high levels of mRNA or protein is consistent with the C5-12 promoter being less active in atria. However, another possible explanation is that the VG were simply not cleared due to the short timeline of this study. More experiments are needed to better understand the relative activities as this can impact dose projections.

Each cardiac and skeletal muscle disease will have its own expression requirements to achieve efficacy. For DMD, approximately 20% of mini-dystrophin protein levels lead to substantial efficacy in transgenic mice when the protein is expressed in every cell. Here, delivery of 1.18×10^{14} VG/kg of AAV8-microdystrophin-FLAG led to 20% wild-type dystrophin protein levels in approximately 30%–50% of skeletal muscle fibers and 17% of left ventricle cardiac cells. Pre-clinical and clinical studies predict that expression as low as ∼5% can lead to efficacy and that 15% of normal levels of dystrophin in all muscle cells can prevent dystrophic pathology, depending on the functionality of the truncated dystrophin.[3,30,42–48] More localized delivery methods such as intramuscular injection and isolated limb perfusion can achieve much greater levels of expression,[31] but these localized delivery methods are not ideal for treating the vast muscle mass in humans. This study also serves as the basis for comparing capsid evolution efforts, which are already showing great promise in reaching more striated muscles with lower doses in NHPs.[49–51]

MATERIALS AND METHODS

AAV production

AAV5 was manufactured using the BEVS, as previously described (US Patent 10837027).[32,33] AAV8 and AAV9 were generated using the same methods, except that the AAV8 or AAV9 (hu.14) *CAP* genes were utilized instead of the AAV5 *CAP* gene. The DNA expression cassette contained a C5-12 promoter, a microdystrophin-FLAG transgene that has previously been demonstrated to be safe in NHPs when systemically delivered at high doses,[31] and a synthetic poly(A) within the ITRs, totaling 4,412 bp. The 50-L production runs yielded 2.4×10^{16} VG AAV5-microdystrophin-FLAG (36% full capsids), 3.1×10^{15} VG (25% full capsids) AAV8-microdystrophin-FLAG, and 2.4×10^{16} VG/mL (43% full capsids) AAV9-microdystrophin-FLAG. The production of AAV8 enabled the administration of two monkeys at 1.18×10^{14} VG/kg, whereas the

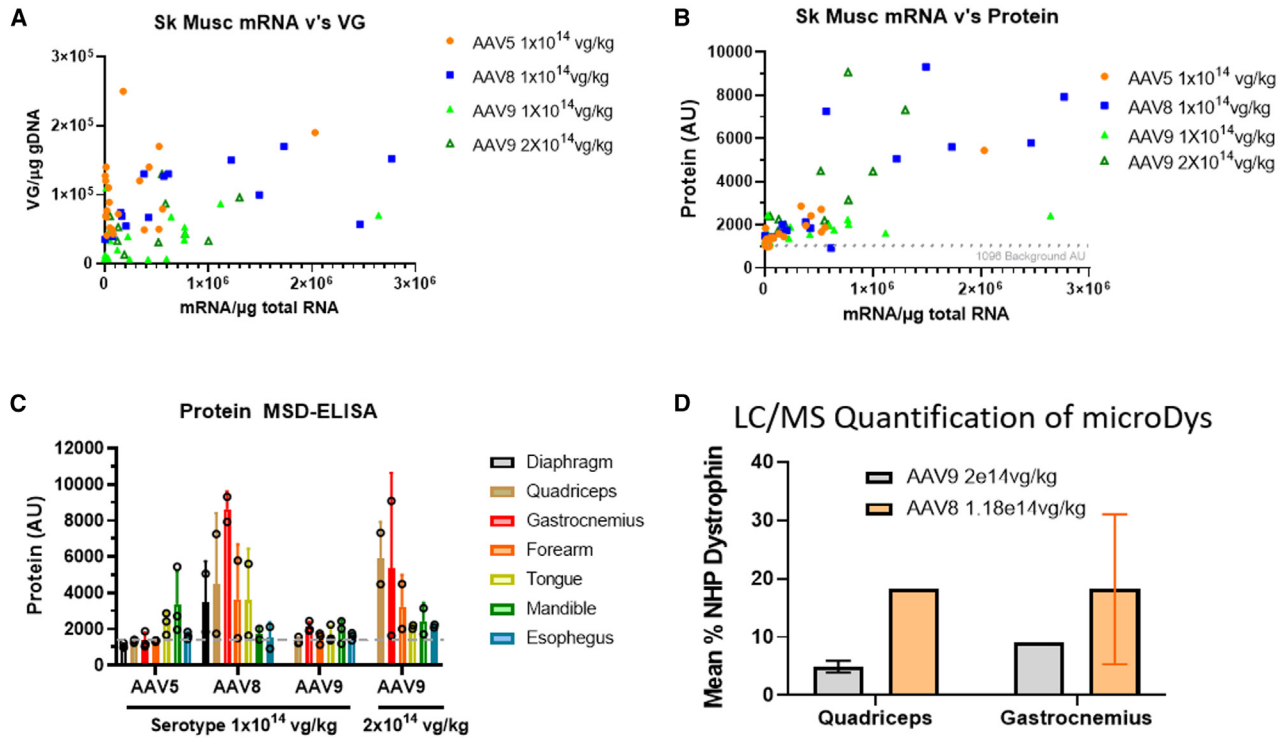

Figure 3. Expression and biodistribution in the skeletal muscles after systemic delivery of AAV-C5-12-micordystrophin-FLAG

(A) The relationship of VG/µg gDNA versus mRNA/µg total RNA for each sample. Note that the AAV8 samples shown in blue have more mRNA. (B) The relationship of MSD-ELISA-quantified microdystrophin-FLAG protein levels versus mRNA/µg total RNA for each sample. The dashed line shows the average background arbitrary units from the MSD-ELISA. Note that the AAV8 levels in blue have more mRNA and protein than AAV5 or AAV9. (C) The mean ± SD MSD-ELISA protein levels from each skeletal muscle. (D) LC-MS quantification of microdystrophin-FLAG protein as a percentage of wild-type NHP dystrophin.

production of AAV9 enabled the treatment of three monkeys at 1.18×10^{14} VG/kg and two monkeys at 2×10^{14} VG/kg. The endotoxin units (EU) were each below 0.1 EU/mL, with a bioburden less than 1. The vectors were formulated in 1× PBS (minus Ca^{2+} and Mg^{2+}), 5% sucrose, and 0.02% Tween 20 and stored at −80°C.

nAbs

Cynomolgus monkeys (*M. fascicularis*) were selected for low total and nAbs. Serum samples were flash frozen in liquid N_2, shipped on dry ice, and stored in a −80°C freezer until analysis. Serum from 15 pre- and post-test NHPs were examined for AAV5, AAV8, and AAV9 tAbs and nAbs, as previously described.[52] Total antibody assessments were performed using an ELISA. Briefly, the method consisted of coating 96-well polypropylene plates overnight with purified AAV5, AAV8, or AAV9 capsids at ∼4 µg/mL each. A purified monkey immunoglobulin G (IgG) was used as a positive control. Blocked and washed plates were probed the following day with a serial dilution of the serum samples and detected with horseradish peroxidase-labeled anti-monkey IgG detection Abs. Background signal was detected in wells without serum incubation. In total, two experimental runs were performed: one for the detection of Abs in pre-treatment samples and another for post-treatment samples. Treatment emergent tAbs were assessed by comparing raw data units obtained in the ELISA for post-treatment samples with the raw data units of respective pre-treatment samples. In the total Ab assay, all results above background were accepted. Assay precision (percent CV [coefficient of variation]) was evaluated for replicate samples where applicable. In general, percent CV was shown to be <20%. For nAb assays, percent CV was shown to be <35%. However, in 8% of the samples, CVs were >35% because one of the replicates was close to noise. Results from the nAb assay are shown as % of negative control, and data were accepted when the positive controls (positive quality assay $\leq$50%) respect to negative quality control. A 50% cut point was used to determine whether a sample was positive. Test samples with an average percentage of <50% were considered positive for the nAb response.

NHPs and dosing

A total of 10 NHPs with low tAbs and nAbs were selected for dosing with AAV. Methylprednisolone acetate was intramuscularly dosed at 2 mg/kg to all animals from days 0 to 3 post-AAV administration to mitigate any potential compound side effects. NHPs also received an oral dose of 5 mg famotidine 0–3 days post-AAV administration to inhibit gastric acid production during steroid administration to mitigate potential treatment-related inappetence. This was a single-dose exploratory intravenous study in monkeys with a 4-week post-dose

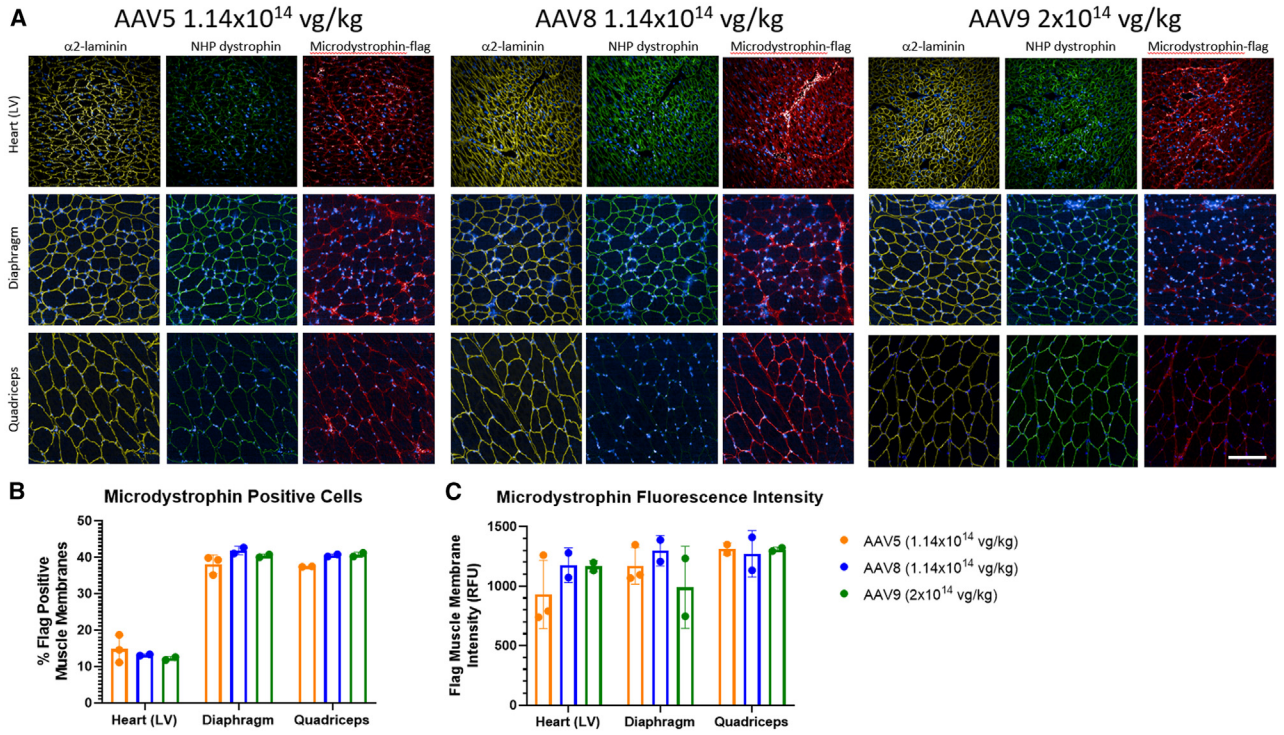

Figure 4. Microdystrophin-FLAG cellular distribution

(A) Representative examples of microdystrophin-FLAG immunostaining in the sarcolemma of NHP quadriceps muscle treated with AAV5, AAV8, or AAV9 C5-12-microdystrophin-FLAG. Scale bar, 100 μm. (B) The mean ± SD proportion of left ventricle, diaphragm, and quadriceps muscle membranes expressing microdystrophin-FLAG. (C) The mean ± SD fluorescence intensity of left ventricle, diaphragm, and quadriceps muscle membranes expressing microdystrophin-FLAG.

recovery. We compared $n = 3$ NHPs with 1.18×10^{14} VG/kg AAV5, $n = 2$ NHPs with 1.18×10^{14} VG/kg AAV8, $n = 3$ NHPs with 1.18×10^{14} VG/kg AAV9, and $n = 2$ NHPs with 2×10^{14} VG/kg AAV9. The vector was thawed at 4°C for up to 24 h prior to dosing. The vectors were not diluted prior to dosing a maximum volume of 7.5 mL/kg bolus infusion. All animal research was internally reviewed and approved by the BMS Institutional Animal Care and Use Committee (IACUC).

gDNA isolation and qPCR for plasma toxicokinetics

DNA was extracted from 0.5 mL plasma collected at 1, 4, 7, 24, and 48 h after dosing using the DNeasy Blood and Tissue Kit (Qiagen) as per the manufacturer's protocol. The DNA concentrations were measured with the Nanodrop 8000. Each microdystrophin-FLAG tag sample was run in duplicate with primer/probe sets (forward primer 5′-AACGCTCAGTTCAGCAAATTTG-3′; reverse primer 5′-CCTGCAGGTCGGAAAACAGA-3′; probe-6FAM-AAGCAGCACATCGAG-MGBNFQ) in 384-well clear reaction plates (Applied Biosystems, catalog no. 4483285). To each reaction, 2 μL gDNA (80 ng) and 8 μL master mix (5 μL Fast Advanced Master Mix, 0.5 μL 20× FAM primer probe mix, and 2.5 μL water) were added, and plates were centrifuged for 1 min at 1,000 rpm. Samples were incubated at 95°C for 10 min, followed by 40 cycles at 95°C for 15 s and 60°C for 1 min using the ViiA7 system and Quant Studio real-time PCR software for data analysis (Applied Biosystems). Plasma microdystrophin DNA was quantified by qPCR using linearized plasmid DNA (13,176 bp; 1 ng = 7×10^7 copies) as a standard.

VG biodistribution in tissues

For gDNA isolation, heart, skeletal muscle, liver, kidney, and lung tissues were homogenized using Qiagen TissueLyser II (catalog no. 85300), and gDNA was isolated using a Qiagen DNeasy 96 blood and tissue kit (catalog no. 69581). Tissue samples (~20 mg each) were placed in 96-well plates (costar assay block 1 mL, catalog no. 3958) containing 200 μL Proteinase K-buffer ATL and one 5-mm steel bead, homogenized using TissueLyser II at 30 Hz for 2 min, and repeat until it was homogenized. gDNA was isolated following the manufacturer's instructions. DNA concentrations were measured by Nanodrop 8000. For qPCR, each sample was run in duplicate with primer/probe sets (forward primer 5′-AACGCTCAGTTCAGCAAATTTG-3′; reverse primer 5′-CCTGCAGGTCGGAAAACAGA-3′; probe-6FAM-AAGCAGCACATCG-AG-MGBNFQ) in 384-well clear reaction plates (Applied Biosystems, catalog no. 4483285). To each reaction, 2 μL gDNA (80 ng) and 8 μL master mix (5 μL Fast Advanced Master Mix, 0.5 μL 20× FAM primer probe mix, and 2.5 μL water) were added, and plates were centrifuged for 1 min at 1,000 rpm. Samples were incubated at 95°C for 10 min, followed by

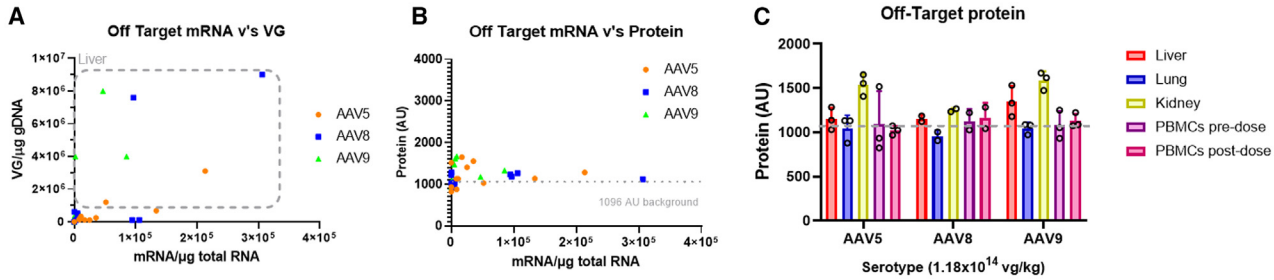

Figure 5. Expression in off-target tissues

(A) The relationship of VG/µg gDNA versus mRNA/µg total RNA for each sample. Dashed box shows the liver samples with high VG levels but low mRNA levels. (B) The relationship of MSD-ELISA quantified microdystrophin-FLAG protein levels versus mRNA/µg total RNA for each sample. The dashed line shows the average background arbitrary units from the MSD-ELISA. Note that the AAV8 levels in blue have more mRNA and protein than AAV5 or AAV9. (C) The mean ± SD MSD-ELISA protein levels from each off-target tissue. Note that the kidney has low levels of microdystrophin-FLAG protein marginally above background.

40 cycles at 95°C for 15 s and 60°C for 1 min using the ViiA7 system and Quant Studio real-time PCR software for data analysis (Applied Biosystems). Plasma microdystrophin DNA was quantified by qPCR using linearized plasmid DNA (13,176 bp; 1 ng = 7 × 10^7 copies) as a standard.

mRNA

For isolation of total RNA, tissues were homogenized using Qiagen TissueLyser II, and RNA was isolated using a Qiagen RNeasy 96 Universal tissue kit (catalog no. 74881). Tissues (∼15 mg each) were placed in RNeasy kit collection microtubes containing 750 µL Qiazol reagent and one 5-mm steel bead (Qiagen, catalog no. 69989), homogenized using TissueLyser II at 30 Hz for 2 min, and this step repeated until homogenized, followed by a centrifugation at 6,000 × *g* for 4 min at 4°C. To each tube, 150 µL chloroform was added, and samples were vortexed vigorously for 15 s. Following a 3-min incubation at room temperature, samples were spun at 6,000 × *g* for 15 min at 4°C. The aqueous phase was removed (∼360 µL) and transferred to a new tube containing 1 vol RNase free 70% EtOH. All samples were transferred to a RNeasy 96-well plate for RNA isolation following the manufacturer's instructions (Qiagen). RNA yield was quantified with the Nanodrop 8000. For cDNA synthesis and subsequent PCR, 1 µg RNA was added to 1 well of a 96-well plate in 10 µL H_2O (Plate-Axygen, PCR-96-C-S). To each well, 10 µL master mix (High Capacity cDNA Reverse Transcription kit, Applied Biosystems) was added, and the plate was centrifuged at 1,000 rpm. cDNA synthesis was carried out at 25°C for 10 min, 37°C for 120 min, and 85°C for 5 min, followed by a hold at 4°C. For qPCR quantification, each sample was run in duplicate with primer/probe sets (forward primer 5′-AACGCTCAGTTC AGCAAATTTG-3'; reverse primer 5′- CTGCAGGTCGGAAAAC AGA -3'; probe-6FAM-AAGCAGCACATCGAG-MGBNFG) in 384-well clear reaction plates (Applied Biosystems, catalog no. 4483285). To each reaction, 2 µL cDNA and 8 µL master mix (5 µL Fast Advanced Master Mix, 0.5 µL 20× FAM primer probe mix, and 2.5 µL water) were added, and plates were centrifuged for 1 min at 1,000 rpm. Samples were incubated at 95°C for 10 min, followed by 40 cycles at 95°C for 15 s and 60°C for 1 min using the ViiA7 system and Quant Studio real-time PCR software for data analysis (Applied Biosystems).

Microdystrophin-FLAG MSD-ELISA

Multi-assay 96-well plate (Meso Scale Discovery, catalog no. L-15xB) was pre-coated with FLAG tag polyclonal antibody (Invitrogen, catalog no. PA1-984B) at a concentration of 10 µg/mL in bicarbonate buffer and incubated at 4°C overnight. The plate was then blocked with 200 µL blocking buffer (5% BSA in PBS; Sigma, catalog no. A7030) for 4 h with shaking at room temperature. Heart, skeletal muscle, liver, kidney, and lung tissues (∼30 mg) were placed in 96-well plates (costar assay block 1 mL, catalog no. 3958) and homogenized in radioimmunoprecipitation assay (RIPA) buffer (Sigma, catalog no. R0278) at a concentration of 1 mg tissue/10 µL RIPA buffer with protease inhibitor cocktail tablets (Roche, catalog no. 04 693 159 001) using Qiagen TissueLyser at 30 Hz for 5 min, repeating until homogenized. Tissue RIPA lysate was diluted 2-fold in a binding buffer (1% BSA, 0.05% Tween 20, 20 mM Tris, pH 7.5 in PBS). To each well, 40 µL tissue lysates and sulfo-conjugated Manex1011b (10 µg/mL; Developmental Studies Hybridoma Bank) were added to the pre-coated 96-well plates and incubated at 4°C with shaking overnight. The plate was washed three times with PBS containing 0.05% Tween 20 (Bio-Rad, catalog no. 161-0781) and 150 µL MSD read buffer T with surfactant was added (Meso Scale Discovery, catalog no. R92TC-1). The plate was then read on the MSD Sector 6000 machine.

Microdystrophin-FLAG LC-MS

Heart, skeletal muscle, liver, lung, and kidney were collected and immediately frozen. Prior to analyses, the tissues were homogenized with RIPA buffer (fortified to 1% SDS for cynomolgus monkey samples) in a 1:10 ratio. The homogenates were digested with trypsin, and after fractionation for peptide enrichment, the samples were analyzed by LC-MS/MS by monitoring previously identified unique peptides corresponding to the endogenous cynomolgus monkey dystrophin (MEAWLENFAR) and the dosed human microdystrophin (TEAWLDNFAR). Stable isotope labeled (SIL) analogs for human

and/or cynomolgus monkey peptides were spiked into the homogenate and were used to estimate the measured levels. Total protein was also obtained and used for normalization purposes.

Proportion of microdystrophin-FLAG$^+$ cells

Heart, skeletal muscle, liver, kidney, and lung tissues were frozen in Optimal cutting temperature and sectioned in 5-μm slices on standard microscope slides. On the day of staining, frozen tissue slides were removed from the −80°C freezer and allowed to warm to room temperature. Slides were blocked with 200 μL blocking buffer (Dulbecco's phosphate-buffered saline [DPBS], Thermo Fisher, catalog no. 14190144) supplemented with 0.05% Triton X-100 (Sigma, catalog no. T8787) and 1% BSA (Sigma, catalog no.A9576) for 30 min. Three primary antibodies were diluted in blocking buffer, including the Alexa 488 conjugated mandys106 (1:200) rabbit anti-FLAG antibody (1:500; Thermo Fisher, catalog no. PA1-984B) and a rat anti-laminin-2 antibody (1:500; Sigma, catalog no. L0663). Blocking buffer was removed with a vacuum aspirator, and primary antibody was added to each slide. Following a 1-h incubation at room temperature, slides were washed three times in DPBS. Two secondary antibodies were diluted in blocking buffer, including an Alexa Fluor 546 goat anti-rat antibody (Thermo Fisher, catalog no. A11077) and an Alexa Fluor 647 goat anti-rabbit (Thermo Fisher, catalog no. A21244). DAPI was also included in the secondary antibody solution to counterstain nuclei in the tissue. Secondary antibody was added to the tissue and incubated for 30 min at room temperature. Following the staining protocol, slides were washed three times with DPBS followed by a rinse with distilled H_2O. One drop of ProLong diamond antifade mountant (Thermo Fisher, catalog no. P36962) was added to seal the coverslip on the tissue. Slides were saved at 4°C for imaging the next day. Image acquisition of the microscope slide was conducted on the Opera Phenix HCS imager (PerkinElmer) equipped with a laser microlens confocal and large 4.7 megapixel complementary metal oxide semiconductor camera. Fluorescent dyes used for labeling tissues were matched with the appropriate laser excitation light sources and complementary emission filters—nucleus (DAPI): excitation 375 nm, emission 435–480 nm; mini-dystrophin (Alexa Fluor 647): ex 640 nm, em 650–760 nm; and laminin (Alexa Fluor 546): ex 561 nm, em 570–630 nm. The software package Harmony 4.9 was used for image acquisition. The software first performed a low-magnification scan at 5× to identify the region of interest (ROI). A second round of multi-color image acquisition on the ROI was performed using a water objective lens at 20× magnification. A montage image of the ROI was captured with 20% overlap between fields of view. Images were imported into the Columbus image management system for analysis and quantitation. A building block analysis routine was created in Columbus to identify muscle fibers in both heart and skeletal muscle tissue and quantitate the amount of FLAG staining. A global image of the entire tissue was created. Each field of view was inverted so that the software could identify "cells" that were outlined with laminin stain. Size and intensity filters were applied to identify only true muscle fibers. The outer membrane of the laminin stain was dilated, and the microdystrophin-FLAG intensity inside this region was calculated (Figure S3). Intensities were calculated for all tissues for all animal groups. Intensity cutoffs for "cells" or muscle fibers positive for dystrophin were determined for each tissue slice from each animal, using a mean intensity plus 3 standard deviations (SDs) calculations.

DATA AND CODE AVAILABILITY

The data presented in this study can be made available upon request from Bristol Myers Squibb (BMS).

ACKNOWLEDGMENTS

We would sincerely like to thank Dike Qiu, Uma Kavita and the BMS veterinary staff and toxicology department for their help with this study.

AUTHOR CONTRIBUTIONS

M.L. processed the tissues and examined VG, mRNA, and MSD-ELISA assays. E.C., Z.L., and G.B.B. designed and performed the biodistribution studies. Y.D. performed the nAb and tAb studies. E.E., F.d.P., and J.L. generated the AAV using BEVS. B.G.S. and P.S. designed and performed the LC-MS. J.G., P.C.L., and G.B.B. organized the NHP study. D.G., L.P.A., and G.B.B. reviewed and approved the design of the studies. G.B.B. designed the constructs, the overall study design, and wrote the manuscript. All authors contributed to the writing and review of the manuscript.

DECLARATION OF INTERESTS

All BMS current and/or previous employees hold BMS stock, and all previous uniQure employees hold uniQure stock and each has various commercial interests in developing gene therapies.

SUPPLEMENTAL INFORMATION

Supplemental information can be found online at https://doi.org/10.1016/j.omtm.2025.101411.

REFERENCES

1. Dunbar, C.E., High, K.A., Joung, J.K., Kohn, D.B., Ozawa, K., and Sadelain, M. (2018). Gene therapy comes of age. Science *359*, eaan4672. https://doi.org/10.1126/science.aan4672.

2. Samulski, R.J., and Muzyczka, N. (2014). AAV-Mediated Gene Therapy for Research and Therapeutic Purposes. Annu. Rev. Virol. *1*, 427–451. https://doi.org/10.1146/annurev-virology-031413-085355.

3. Duan, D. (2018). Systemic AAV Micro-dystrophin Gene Therapy for Duchenne Muscular Dystrophy. Mol. Ther. *26*, 2337–2356. https://doi.org/10.1016/j.ymthe.2018.07.011.

4. Ishikawa, K., Weber, T., and Hajjar, R.J. (2018). Human Cardiac Gene Therapy. Circ. Res. *123*, 601–613. https://doi.org/10.1161/CIRCRESAHA.118.311587.

5. Crudele, J.M., and Chamberlain, J.S. (2019). AAV-based gene therapies for the muscular dystrophies. Hum. Mol. Genet. *28*, R102–R107. https://doi.org/10.1093/hmg/ddz128.

6. Cannata, A., Ali, H., Sinagra, G., and Giacca, M. (2020). Gene Therapy for the Heart Lessons Learned and Future Perspectives. Circ. Res. *126*, 1394–1414. https://doi.org/10.1161/CIRCRESAHA.120.315855.

7. Kuzmin, D.A., Shutova, M.V., Johnston, N.R., Smith, O.P., Fedorin, V.V., Kukushkin, Y.S., van der Loo, J.C.M., and Johnstone, E.C. (2021). The clinical landscape for AAV gene therapies. Nat. Rev. Drug Discov. *20*, 173–174. https://doi.org/10.1038/d41573-021-00017-7.

8. Chamberlain, J.S. (2022). A Boost for Muscle with Gene Therapy. N. Engl. J. Med. *386*, 1184–1186. https://doi.org/10.1056/NEJMcibr2118576.

9. Baldrick, P., McIntosh, B., and Prasad, M. (2023). Adeno-associated virus (AAV)-based gene therapy products: What are toxicity studies in non-human primates showing us? Regul. Toxicol. Pharmacol. *138*, 105332. https://doi.org/10.1016/j.yrtph.2022.105332.

10. Singh, M., Brooks, A., Toofan, P., and McLuckie, K. (2024). Selection of appropriate non-clinical animal models to ensure translatability of novel AAV-gene therapies to the clinic. Gene Ther. *31*, 56–63. https://doi.org/10.1038/s41434-023-00417-x.

11. Zincarelli, C., Soltys, S., Rengo, G., and Rabinowitz, J.E. (2008). Analysis of AAV serotypes 1-9 mediated gene expression and tropism in mice after systemic injection. Mol. Ther. *16*, 1073–1080. https://doi.org/10.1038/mt.2008.76.

12. Faust, S.M., Bell, P., Cutler, B.J., Ashley, S.N., Zhu, Y., Rabinowitz, J.E., and Wilson, J.M. (2013). CpG-depleted adeno-associated virus vectors evade immune detection. J. Clin. Invest. *123*, 2994–3001. https://doi.org/10.1172/JCI68205.

13. Srivastava, A. (2016). In vivo tissue-tropism of adeno-associated viral vectors. Curr. Opin. Virol. *21*, 75–80. https://doi.org/10.1016/j.coviro.2016.08.003.

14. Muhuri, M., Maeda, Y., Ma, H., Ram, S., Fitzgerald, K.A., Tai, P.W., and Gao, G. (2021). Overcoming innate immune barriers that impede AAV gene therapy vectors. J. Clin. Invest. *131*, e143780. https://doi.org/10.1172/JCI143780.

15. Pupo, A., Fernández, A., Low, S.H., François, A., Suárez-Amarán, L., and Samulski, R.J. (2022). AAV vectors: The Rubik's cube of human gene therapy. Mol. Ther. *30*, 3515–3541. https://doi.org/10.1016/j.ymthe.2022.09.015.

16. Pan, X., Yue, Y., Zhang, K., Hakim, C.H., Kodippili, K., McDonald, T., and Duan, D. (2015). AAV-8 is more efficient than AAV-9 in transducing neonatal dog heart. Hum. Gene Ther. Methods *26*, 54–61. https://doi.org/10.1089/hgtb.2014.128.

17. Mendell, J.R., Sahenk, Z., Lehman, K., Nease, C., Lowes, L.P., Miller, N.F., Iammarino, M.A., Alfano, L.N., Nicholl, A., Al-Zaidy, S., et al. (2020). Assessment of Systemic Delivery of rAAVrh74.MHCK7.micro-dystrophin in Children With Duchenne Muscular Dystrophy: A Nonrandomized Controlled Trial. JAMA Neurol. *77*, 1122–1131. https://doi.org/10.1001/jamaneurol.2020.1484.

18. Yadin, D., Guetta, T., Petrover, Z., Alcalai, R., Seidman, J., Seidman, C.E., Ofek, E., Kornowski, R., Hochhauser, E., and Arad, M. (2023). Effect of pharmacological heart failure drugs and gene therapy on Danon's cardiomyopathy. Biochem. Pharmacol. *215*, 115735. https://doi.org/10.1016/j.bcp.2023.115735.

19. Chiorini, J.A., Kim, F., Yang, L., and Kotin, R.M. (1999). Cloning and characterization of adeno-associated virus type 5. J. Virol. *73*, 1309–1319. https://doi.org/10.1128/JVI.73.2.1309-1319.1999.

20. Miesbach, W., Meijer, K., Coppens, M., Kampmann, P., Klamroth, R., Schutgens, R., Tangelder, M., Castaman, G., Schwäble, J., Bonig, H., et al. (2018). Gene therapy with adeno-associated virus vector 5-human factor IX in adults with hemophilia B. Blood *131*, 1022–1031. https://doi.org/10.1182/blood-2017-09-804419.

21. Klamroth, R., Hayes, G., Andreeva, T., Gregg, K., Suzuki, T., Mitha, I.H., Hardesty, B., Shima, M., Pollock, T., Slev, P., et al. (2022). Global Seroprevalence of Pre-existing Immunity Against AAV5 and Other AAV Serotypes in People with Hemophilia A. Hum. Gene Ther. *33*, 432–441. https://doi.org/10.1089/hum.2021.287.

22. Li, X., Eastman, E.M., Schwartz, R.J., and Draghia-Akli, R. (1999). Synthetic muscle promoters: activities exceeding naturally occurring regulatory sequences. Nat. Biotechnol. *17*, 241–245. https://doi.org/10.1038/6981.

23. Salva, M.Z., Himeda, C.L., Tai, P.W., Nishiuchi, E., Gregorevic, P., Allen, J.M., Finn, E.E., Nguyen, Q.G., Blankinship, M.J., Meuse, L., et al. (2007). Design of tissue-specific regulatory cassettes for high-level rAAV-mediated expression in skeletal and cardiac muscle. Mol. Ther. *15*, 320–329. https://doi.org/10.1038/sj.mt.6300027.

24. Wang, B., Li, J., Fu, F.H., Chen, C., Zhu, X., Zhou, L., Jiang, X., and Xiao, X. (2008). Construction and analysis of compact muscle-specific promoters for AAV vectors. Gene Ther. *15*, 1489–1499. https://doi.org/10.1038/gt.2008.104.

25. Himeda, C.L., Chen, X., and Hauschka, S.D. (2011). Design and testing of regulatory cassettes for optimal activity in skeletal and cardiac muscles. Methods Mol. Biol. *709*, 3–19. https://doi.org/10.1007/978-1-61737-982-6_1.

26. Potter, R.A., Griffin, D.A., Heller, K.N., Peterson, E.L., Clark, E.K., Mendell, J.R., and Rodino-Klapac, L.R. (2021). Dose-Escalation Study of Systemically Delivered rAAVrh74.MHCK7.micro-dystrophin in the mdx Mouse Model of Duchenne Muscular Dystrophy. Hum. Gene Ther. *32*, 375–389. https://doi.org/10.1089/hum.2019.255.

27. Himeda, C.L., Jones, T.I., and Jones, P.L. (2024). Have a little heart (or not): highly minimized skeletal muscle regulatory cassettes with low or no activity in heart. Hum. Gene Ther. *35*, 543–554. https://doi.org/10.1089/hum.2024.041.

28. Skopenkova, V.V., Egorova, T.V., and Bardina, M.V. (2021). Muscle-Specific Promoters for Gene Therapy. Acta Naturae *13*, 47–58. https://doi.org/10.32607/actanaturae.11063.

29. Duan, D., Goemans, N., Takeda, S., Mercuri, E., and Aartsma-Rus, A. (2021). Duchenne muscular dystrophy. Nat. Rev. Dis. Prim. *7*, 13. https://doi.org/10.1038/s41572-021-00248-3.

30. Harper, S.Q., Hauser, M.A., DelloRusso, C., Duan, D., Crawford, R.W., Phelps, S.F., Harper, H.A., Robinson, A.S., Engelhardt, J.F., Brooks, S.V., and Chamberlain, J.S. (2002). Modular flexibility of dystrophin: implications for gene therapy of Duchenne muscular dystrophy. Nat. Med. *8*, 253–261. https://doi.org/10.1038/nm0302-253.

31. Rodino-Klapac, L.R., Montgomery, C.L., Bremer, W.G., Shontz, K.M., Malik, V., Davis, N., Sprinkle, S., Campbell, K.J., Sahenk, Z., Clark, K.R., et al. (2010). Persistent expression of FLAG-tagged micro dystrophin in nonhuman primates following intramuscular and vascular delivery. Mol. Ther. *18*, 109–117. https://doi.org/10.1038/mt.2009.254.

32. Kotin, R.M. (2011). Large-scale recombinant adeno-associated virus production. Hum. Mol. Genet. *20*, R2–R6. https://doi.org/10.1093/hmg/ddr141.

33. Bosma, B., du Plessis, F., Ehlert, E., Nijmeijer, B., de Haan, M., Petry, H., and Lubelski, J. (2018). Optimization of viral protein ratios for production of rAAV serotype 5 in the baculovirus system. Gene Ther. *25*, 415–424. https://doi.org/10.1038/s41434-018-0034-7.

34. Gregorevic, P., Meznarich, N.A., Blankinship, M.J., Crawford, R.W., and Chamberlain, J.S. (2008). Fluorophore-labeled myosin-specific antibodies simplify muscle-fiber phenotyping. Muscle Nerve *37*, 104–106. https://doi.org/10.1002/mus.20877.

35. Gregorevic, P., Blankinship, M.J., Allen, J.M., Crawford, R.W., Meuse, L., Miller, D.G., Russell, D.W., and Chamberlain, J.S. (2004). Systemic delivery of genes to striated muscles using adeno-associated viral vectors. Nat. Med. *10*, 828–834. https://doi.org/10.1038/nm1085.

36. Denard, J., Rouillon, J., Leger, T., Garcia, C., Lambert, M.P., Griffith, G., Jenny, C., Camadro, J.M., Garcia, L., and Svinartchouk, F. (2018). AAV-8 and AAV-9 Vectors Cooperate with Serum Proteins Differently Than AAV-1 and AAV-6. Mol. Ther. Methods Clin. Dev. *10*, 291–302. https://doi.org/10.1016/j.omtm.2018.08.001.

37. Issa, S.S., Shaimardanova, A.A., Solovyeva, V.V., and Rizvanov, A.A. (2023). Various AAV Serotypes and Their Applications in Gene Therapy: An Overview. Cells *12*, 785. https://doi.org/10.3390/cells12050785.

38. Ramos, J.N., Hollinger, K., Bengtsson, N.E., Allen, J.M., Hauschka, S.D., and Chamberlain, J.S. (2019). Development of Novel Micro-dystrophins with Enhanced Functionality. Mol. Ther. *27*, 623–635. https://doi.org/10.1016/j.ymthe.2019.01.002.

39. Banks, G.B., Chamberlain, J.S., and Odom, G.L. (2020). Microutrophin expression in dystrophic mice displays myofiber type differences in therapeutic effects. PLoS Genet. *16*, e1009179. https://doi.org/10.1371/journal.pgen.1009179.

40. Le Guiner, C., Servais, L., Montus, M., Larcher, T., Fraysse, B., Moullec, S., Allais, M., François, V., Dutilleul, M., Malerba, A., et al. (2017). Long-term microdystrophin gene therapy is effective in a canine model of Duchenne muscular dystrophy. Nat. Commun. *8*, 16105. https://doi.org/10.1038/ncomms16105.

41. Sarcar, S., Tulalamba, W., Rincon, M.Y., Tipanee, J., Pham, H.Q., Evens, H., Boon, D., Samara-Kuko, E., Keyaerts, M., Loperfido, M., et al. (2019). Next-generation muscle-directed gene therapy by in silico vector design. Nat. Commun. *10*, 492. https://doi.org/10.1038/s41467-018-08283-7.

42. Hoffman, E.P., Fischbeck, K.H., Brown, R.H., Johnson, M., Medori, R., Loike, J.D., Harris, J.B., Waterston, R., Brooke, M., Specht, L., et al. (1988). Characterization of dystrophin in muscle-biopsy specimens from patients with Duchenne's or Becker's muscular dystrophy. N. Engl. J. Med. *318*, 1363–1368. https://doi.org/10.1056/NEJM198805263182104.

43. Hoffman, E.P., Kunkel, L.M., Angelini, C., Clarke, A., Johnson, M., and Harris, J.B. (1989). Improved diagnosis of Becker muscular dystrophy by dystrophin testing. Neurology *39*, 1011–1017.

44. Beggs, A.H., Hoffman, E.P., Snyder, J.R., Arahata, K., Specht, L., Shapiro, F., Angelini, C., Sugita, H., and Kunkel, L.M. (1991). Exploring the molecular basis for variability

among patients with Becker muscular dystrophy: dystrophin gene and protein studies. Am. J. Hum. Genet. *49*, 54–67.

45. Byers, T.J., Neumann, P.E., Beggs, A.H., and Kunkel, L.M. (1992). ELISA quantitation of dystrophin for the diagnosis of Duchenne and Becker muscular dystrophies. Neurology *42*, 570–576.

46. Wells, D.J., Wells, K.E., Asante, E.A., Turner, G., Sunada, Y., Campbell, K.P., Walsh, F.S., and Dickson, G. (1995). Expression of human full-length and minidystrophin in transgenic mdx mice: implications for gene therapy of Duchenne muscular dystrophy. Hum. Mol. Genet. *4*, 1245–1250.

47. Li, D., Yue, Y., and Duan, D. (2008). Preservation of muscle force in Mdx3cv mice correlates with low-level expression of a near full-length dystrophin protein. Am. J. Pathol. *172*, 1332–1341. https://doi.org/10.2353/ajpath.2008.071042.

48. Godfrey, C., Muses, S., McClorey, G., Wells, K.E., Coursindel, T., Terry, R.L., Betts, C., Hammond, S., O'Donovan, L., Hildyard, J., et al. (2015). How much dystrophin is enough: the physiological consequences of different levels of dystrophin in the mdx mouse. Hum. Mol. Genet. *24*, 4225–4237. https://doi.org/10.1093/hmg/ddv155.

49. Weinmann, J., Weis, S., Sippel, J., Tulalamba, W., Remes, A., El Andari, J., Herrmann, A.K., Pham, Q.H., Borowski, C., Hille, S., et al. (2020). Identification of a myotropic AAV by massively parallel in vivo evaluation of barcoded capsid variants. Nat. Commun. *11*, 5432. https://doi.org/10.1038/s41467-020-19230-w.

50. Tabebordbar, M., Lagerborg, K.A., Stanton, A., King, E.M., Ye, S., Tellez, L., Krunnfusz, A., Tavakoli, S., Widrick, J.J., Messemer, K.A., et al. (2021). Directed evolution of a family of AAV capsid variants enabling potent muscle-directed gene delivery across species. Cell *184*, 4919–4938.e22. https://doi.org/10.1016/j.cell.2021.08.028.

51. El Andari, J., Renaud-Gabardos, E., Tulalamba, W., Weinmann, J., Mangin, L., Pham, Q.H., Hille, S., Bennett, A., Attebi, E., Bourges, E., et al. (2022). Semirational bioengineering of AAV vectors with increased potency and specificity for systemic gene therapy of muscle disorders. Sci. Adv. *8*, eabn4704. https://doi.org/10.1126/sciadv.abn4704.

52. Dai, Y., Kavita, U., Lampen, M.H., Gielen, S., Banks, G., Levesque, P., Kozhich, A., Pillutla, R., Zhang, Y., Jawa, V., and Adam, L. (2022). Prevalence of Pre-Existing Neutralizing Antibodies Against Adeno-Associated Virus Serotypes 1, 2, 5, 6, 8, and 9 in Sera of Different Pig Strains. Hum. Gene Ther. *33*, 451–459. https://doi.org/10.1089/hum.2021.213.